

**Supplementary Information**  
**for**  
**Zn(II)-driven impact of monomeric transthyretin on amyloid- $\beta$  amyloidogenesis**

Yelim Yi,<sup>a</sup> Bokyung Kim,<sup>b</sup> Mingeun Kim,<sup>a</sup> Young Ho Ko,<sup>c</sup> Jin Hae Kim<sup>\*b</sup> and Mi Hee Lim<sup>\*a</sup>

<sup>a</sup>Department of Chemistry, Korea Advanced Institute of Science and Technology (KAIST),  
Daejeon 34141, Republic of Korea

<sup>b</sup>Department of New Biology, Daegu Gyeongbuk Institute of Science and Technology (DGIST),  
Daegu 42988, Republic of Korea

<sup>c</sup>Center for van der Waals Quantum Solids, Institute for Basic Science, Pohang 37673, Republic  
of Korea

\*To whom correspondence should be addressed: [miheelim@kaist.ac.kr](mailto:miheelim@kaist.ac.kr) and  
[jinhaekim@dgist.ac.kr](mailto:jinhaekim@dgist.ac.kr)

## Table of Contents

### Experimental Section

Materials and Methods	S4
Preparation of Monomeric Transthyretin (M-TTR)	S4
Preparation of Amyloid- $\beta$ ( $A\beta$ )	S5
Thioflavin-T (ThT) Assay	S6
Transmission Electron Microscopy (TEM)	S7
Cell Viability Studies	S7
Electronic Absorption (Abs) Spectroscopy	S8
Two-dimensional $^1\text{H}$ - $^{15}\text{N}$ Heteronuclear Single Quantum Coherence Nuclear Magnetic Resonance (2D $^1\text{H}$ - $^{15}\text{N}$ HSQC NMR) Spectroscopy	S8
Electrospray Ionization–Mass Spectrometry (ESI–MS), Tandem MS (ESI–MS <sup>2</sup> ), and Liquid Chromatography–MS (LC–MS)	S9
Cross-linking Experiments	S9
<b>Table S1</b> Fitting parameters and mean squared residual error obtained from the global fitting of kinetic models to the experimental data shown in Fig. 1c and S6	S11
<b>Fig. S1</b> Aggregation kinetics of M-TTR with and without Zn(II) treatment monitored by the ThT assay	S12
<b>Fig. S2</b> Aggregation profile of $A\beta_{40}$ in the presence of equimolar Zn(II)	S13
<b>Fig. S3</b> Normalized aggregation curves of $A\beta_{40}$ in the presence of equimolar Zn(II) with the global fitting of the secondary nucleation model involving primary nucleation, elongation, and secondary nucleation steps	S14
<b>Fig. S4</b> Aggregation kinetics of Zn(II)-added $A\beta_{40}$ in the presence of seeds traced by the ThT assay	S15
<b>Fig. S5</b> Aggregation curves of Zn(II)-treated $A\beta_{40}$ in the presence of seeds investigated by the ThT assay	S16
<b>Fig. S6</b> Aggregation kinetics of metal-free $A\beta_{40}$ observed by the ThT assay	S17
<b>Fig. S7</b> Effect of M-TTR on the aggregation kinetics of metal-free $A\beta_{40}$ analyzed by the ThT assay	S18
<b>Fig. S8</b> Change in the combined rate constant, $k+k_n$ , of $A\beta_{40}$ aggregation upon addition of M-TTR without Zn(II) treatment	S19

<b>Fig. S9</b>	Aggregation kinetics of metal-free A $\beta$ <sub>40</sub> in the absence and presence of M-TTR with 35% v/v or 2% v/v seeds	S20
<b>Fig. S10</b>	Change in rate constants ( $k_+$ , $k_n$ and $k_2$ ) of metal-free A $\beta$ <sub>40</sub> aggregation upon treatment of M-TTR obtained from the aggregation curves shown in Fig. S7 and S9b	S21
<b>Fig. S11</b>	Determination of the $K_d$ value for the Zn(II)–Zincon complex	S22
<b>Fig. S12</b>	Titration experiments by electronic Abs spectroscopy to obtain the $K_d$ value and Hill coefficient for Zn(II) binding towards M-TTR	S23
<b>Fig. S13</b>	Interactions of M-TTR with A $\beta$ <sub>40</sub> in the absence and presence of Zn(II)	S24
<b>Fig. S14</b>	M-TTR binding to A $\beta$ <sub>40</sub> in the absence of Zn(II) monitored by ESI–MS and ESI–MS <sup>2</sup>	S25
<b>Fig. S15</b>	Original gel images from Fig. S16	S26
<b>Fig. S16</b>	Size distribution of the cross-linked aggregates of M-TTR and A $\beta$ <sub>40</sub> with or without Zn(II) analyzed by SDS–PAGE with Western blotting using anti-A $\beta$ <sub>40</sub> (6E10) and anti-TTR antibodies	S27
<b>Fig. S17</b>	Mass spectra of A $\beta$ <sub>40</sub> , M-TTR, and A $\beta$ <sub>40</sub> with M-TTR	S28
<b>Fig. S18</b>	Mass spectra of Zn(II)-treated A $\beta$ <sub>40</sub> , M-TTR, and A $\beta$ <sub>40</sub> with M-TTR	S29
<b>Fig. S19</b>	A $\beta$ fragments generated upon treatment of M-TTR with A $\beta$ <sub>40</sub> under Zn(II)-treated and -untreated conditions	S30
<b>Fig. S20</b>	LC–MS analysis of the A $\beta$ <sub>40</sub> sample incubated with M-TTR in the presence of Zn(II)	S31
<b>References</b>		S32

## Experimental Section

**Materials and Methods.** All chemical reagents were purchased from commercial suppliers and used as received unless otherwise stated. Synthetic A $\beta$ <sub>40</sub> (DAEFRHDSGYEVHHQKLVFFAEDV-GSNKGAIIGLMVGGVV) was obtained from Peptide Institute (Osaka, Japan) and purified by high-performance liquid chromatography using YMC Pack ODS-A (YMC, Kyoto, Japan) and Imtakt Cadenza CD-C18 columns (Imtakt, Portland, OR, USA). HEPES [2-(4-(2-hydroxyethyl)piperazin-1-yl)ethanesulfonic acid] was purchased from Sigma-Aldrich (St. Louis, MO, USA). Sodium phosphate and Tris-HCl [tris(hydroxymethyl)aminomethane hydrochloride] were acquired from PanReac AppliChem (Darmstadt, Germany). The buffered solution was prepared in doubly distilled water [ddH<sub>2</sub>O; Milli-Q Direct 16 system (18.2 M $\Omega$ -cm; Merck KGaA, Darmstadt, Germany)]. Trace metal contamination was removed from all solutions used for experiments by treating with Chelex (Sigma-Aldrich) overnight. The samples were prepared using Eppendorf tubes (Eppendorf, Hamburg, Germany) unless otherwise stated. Images obtained by gel/Western blot were visualized by a ChemiDoc MP imaging system (Bio-Rad, Hercules, CA, USA). Morphologies of peptide and protein aggregates produced from the aggregation experiments were taken on a Tecnai F20 transmission electron microscope (FEI Company, Eindhoven, Netherlands; KARA). The absorbance and fluorescence values for cell viability studies and the ThT assay, respectively, were determined by a microplate reader (SpectraMax M5; Molecular Devices, Sunnyvale, CA, USA). Ultrasonication for preparing A $\beta$ <sub>40</sub> seeds was conducted by the Q55 sonicator (Qsonica, Newtown, CT, USA). All samples for the ThT assay were prepared in 96-well black polystyrene plates (Corning, Kennebunk, ME, USA) sealed with a polypropylene sealing tape (Thermo Scientific, Waltham, MA, USA). 2D <sup>1</sup>H–<sup>15</sup>N HSQC NMR spectra of uniformly <sup>15</sup>N-labeled A $\beta$ <sub>40</sub> (rPeptide, Georgia, GA, USA) were collected by an Avance III HD 850 MHz NMR spectrometer equipped with a cryogenic HCN probe (Bruker, Billerica, MA, USA). ESI–MS experiments were performed by an Agilent 6530 Accurate Mass Quadrupole Time-of-Flight mass spectrometer with an ESI source (Agilent, Santa Clara, CA, USA). LC–MS experiments were conducted by a XEVO G2-XS QToF (Waters, Milford, MA, USA; KARA). Electronic absorption (Abs) spectra were recorded on the Agilent 8453 ultraviolet–visible spectrophotometer (Agilent).

**Preparation of M-TTR.** M-TTR (GPTGTGESKCPMLVKVLDVAVRGSPAINVAVHVFRKAADDTW-EPFASGKTSESGELHGLTTEEEFVEGIYKVEIDTKSYWKALGISPMHEHAEVVFTANDSGPRRY TIAAMLSPYSYSTTAVVTNPKE) was recombinantly expressed from *Escherichia coli* (*E. coli*) as a fusion protein with a tobacco etch virus (TEV)-cleavable 6x-His tag at the *N*-terminus. We ensured that the recombinant M-TTR construct does not have any additional amino acids other

than the original sequence. Following the previously reported methods, the proteins were expressed in the *E. coli* M15(pREP4) competent cells that were transformed with the pQE30 vector (Qiagen, Hilden, Germany) encoding M-TTR.<sup>1</sup> The competent cells were inoculated into the Luria-Bertani (LB) broth (3 mL) and diluted into fresh media (1 L). After reaching an optical density of 0.6 at 600 nm, protein expression was induced by isopropyl  $\beta$ -D-1-thiogalactopyranoside (1 mM; PanReac AppliChem, Darmstadt, Germany) at 37 °C overnight. The final cell pellets were obtained with centrifugation at 4,000 g for 20 min at 4 °C and stored at –80 °C until used. The proteins were purified by the resuspension of cell pellets in 20 mM sodium phosphate, pH 7.4, 500 mM NaCl, 30 mM imidazole (PanReac AppliChem). The fully resuspended cells were disrupted by sonication, and the resultant lysate was treated with 0.2 mM phenylmethanesulfonyl fluoride (Sigma-Aldrich) to inactivate possible protease contaminants and centrifuged at 40,000 g for 40 min at 4 °C to remove any insoluble cell debris. The clear supernatant was then applied to a nickel affinity column (HisTrap HP; Cytiva, Marlborough, MA, USA) connected to an ÄKTA prime plus fast protein liquid chromatography (FPLC) system (Cytiva). Target proteins were eluted with the solution of imidazole (30–500 mM). To remove the 6x-His tag, the eluted fractions containing the target proteins were dialyzed at 25 °C overnight in 50 mM Tris-HCl, pH 7.5, 0.5 mM EDTA (ethylenediaminetetraacetic acid; PanReac AppliChem), 1 mM DTT (1,4-dithiothreitol; PanReac AppliChem) followed by incubation with TEV protease under the same conditions. The reaction mixture was re-applied to a HisTrap HP column, from which the flow-through fraction was collected. To remove any metal contaminants and disulfide bonds, EDTA (0.5 mM) and DTT (1 mM) were again added to the fraction. This fraction was finally applied to a gel filtration column (HiLoad 16/60 Superdex 75 column; Cytiva) connected to an ÄKTA go FPLC system (Cytiva) in 20 mM HEPES, pH 7.4, 150 mM NaCl. The final pure sample was concentrated, aliquoted, flash-frozen with liquid nitrogen, and stored at –80 °C until used. The fractions from each purification step were monitored by sodium dodecyl sulfate–polyacrylamide gel electrophoresis (SDS–PAGE). The concentration of M-TTR solution was determined by measuring the absorbance at 280 nm ( $\epsilon = 18,450 \text{ M}^{-1}\text{cm}^{-1}$ ).<sup>2</sup>

**Preparation of A $\beta$ .** A $\beta$ <sub>40</sub> was dissolved in NH<sub>4</sub>OH (1% w/w, aq; Sigma-Aldrich, St. Louis, MO, USA). The solutions were aliquoted, lyophilized overnight, and stored at –80 °C. A stock solution of A $\beta$ <sub>40</sub> was prepared by dissolving the lyophilized peptide with NH<sub>4</sub>OH (1% w/w, aq; 10  $\mu$ L) followed by addition of ddH<sub>2</sub>O, as previously reported.<sup>3</sup> The concentration of the solution containing A $\beta$ <sub>40</sub> was determined by measuring the absorbance at 280 nm ( $\epsilon = 1,450 \text{ M}^{-1}\text{cm}^{-1}$ ).<sup>3</sup>

**ThT assay.** The aggregation kinetics of Zn(II)-added and metal-free A $\beta_{40}$  were analyzed by the ThT assay {ThT = 2-[4-(dimethylamino)phenyl]-3,6-dimethyl-1,3-benzothiazol-3-ium chloride; TCI, Portland, OR, USA}. The samples of A $\beta_{40}$  [10–25  $\mu$ M for Zn(II)-treated conditions; 5–25  $\mu$ M for Zn(II)-untreated conditions] with and without ZnCl $_2$  (10–25  $\mu$ M) were incubated with ThT (25  $\mu$ M) at 37 °C under quiescent conditions in 20 mM HEPES, pH 7.4, 150 mM NaCl. To determine the influence of M-TTR on the aggregation kinetics of Zn(II)–A $\beta_{40}$  and metal-free A $\beta_{40}$  with and without seeds, A $\beta_{40}$  seeds were prepared by incubation of A $\beta_{40}$  (25  $\mu$ M) with and without ZnCl $_2$  (25  $\mu$ M) for 24 h at 37 °C under quiescent conditions in the buffered solution followed by ultrasonication. The aggregation curves of A $\beta_{40}$  (25  $\mu$ M) upon treatment of M-TTR [2–37.5  $\mu$ M under Zn(II)-treated conditions; 0.125–2  $\mu$ M under Zn(II)-untreated conditions] with and without ZnCl $_2$  (25  $\mu$ M) were monitored in the absence and presence of A $\beta_{40}$  seeds (1%–35% v/v). The fluorescence intensity was measured by a microplate reader ( $\lambda_{\text{ex}}$  = 440 nm;  $\lambda_{\text{em}}$  = 490 nm; Molecular Devices). The error bars denote s.e.m. for  $n$  = 9 examined over three independent experiments. The aggregation kinetics were analyzed using the AmyloFit online software.<sup>4</sup> The aggregation curves were normalized to obtain the half-time ( $t_{1/2}$ ) values. The  $t_{1/2}$  values were plotted as a function of [A $\beta_{40}$ ] in a double logarithmic scale, and the scaling exponent ( $\gamma$ ) was determined based on the slope. The aggregation curves of Zn(II)–A $\beta_{40}$  and metal-free A $\beta_{40}$  were well-fitted to the models dominated by nucleation elongation (equation 1)<sup>4</sup> and multistep secondary nucleation (equation 2),<sup>4</sup> respectively. In these models, the fraction of A $\beta_{40}$  aggregates at the time ( $t$ ) is given by the following equations.

$$\frac{M_t}{m_{\text{tot}}} = 1 - \frac{m_0}{m_{\text{tot}}} \left( \frac{1}{\mu} \cosh \left( \sqrt{\frac{n_c}{2}} \mu \lambda t + \nu \right) \right)^{-\frac{2}{n_c}} \quad (\text{equation 1})$$

$$\frac{M_t}{M_\infty} = 1 - \left( 1 - \frac{M_0}{M_\infty} \right) e^{-k_\infty t} \left( \frac{B_- + C_+ e^{k t}}{B_+ + C_+ e^{k t}} \frac{B_+ + C_+}{B_- + C_+} \right)^{\frac{k_\infty}{k}} \quad (\text{equation 2})$$

where the definitions of the parameters are

$$m_{\text{tot}} = m_t + M_t$$

$$\lambda = \sqrt{2k_+ k_n m_0^{n_c}}$$

$$\alpha = \sqrt{\frac{k_+ n_c}{k_n m_0^{n_c}} P_0}$$

$$\mu = \sqrt{1 + \alpha^2}$$

$$\nu = \log(\alpha + \mu)$$

$$\kappa = \sqrt{2m_0k_+ \frac{m_0^{n_c}k_2}{1 + \frac{m_0^{n_c}}{K_M}}}$$

$$C_{\pm} = \frac{k_+P_0}{\kappa} \pm \frac{k_+M_0}{2m_0k_+} \pm \frac{\lambda^2}{2\kappa^2}$$

$$k_{\infty} = \sqrt{(2k_+P_0)^2 - 2A - 4k_+k_2m_{\text{tot}}K_M \frac{\log [K_M]}{n_2}}$$

$$A = -\frac{2k_+k_n m_0^{n_c}}{n_c} - 2k_+k_n m_{\text{tot}}K_M \frac{\log [K_M + m_0^{n_c}]}{n_2} - 2k_+k_2K_M m_0 \left( {}_2F_1 \left[ \frac{1}{n_2}, 1, 1 + \frac{1}{n_2}, -\frac{m_0^{n_2}}{K_M} \right] - 1 \right)$$

$$\bar{k}_{\infty} = \sqrt{k_{\infty}^2 - 2C_+C_- \kappa^2}$$

$$B_{\pm} = \frac{k_{\infty} \pm \bar{k}_{\infty}}{2\kappa}$$

In these relations,  $m$  is the concentration of A $\beta_{40}$  monomer;  $M$  and  $P$  are the aggregate mass and number concentrations, respectively;  $M_{\infty}$  is the mass concentration of aggregates at equilibrium, which is same as  $m_{\text{tot}}$  at relatively long incubation time;  $k_n$ ,  $k_+$ , and  $k_2$  are the rate constants of primary nucleation, elongation, and secondary nucleation, respectively;  $K_M$  is the Michaelis constant for secondary nucleation; and  $n_c$  and  $n_2$  are the reaction orders of primary nucleation and secondary nucleation, respectively. Mean residual error (MRE) was obtained to compare the goodness of different fits or models to the same data set.

**TEM.** A $\beta_{40}$  (25  $\mu\text{M}$ ) and M-TTR (25  $\mu\text{M}$ ) were incubated with or without ZnCl<sub>2</sub> (25  $\mu\text{M}$ ) for 24 h at 37 °C under quiescent conditions in 20 mM HEPES, pH 7.4, 150 mM NaCl. Glow-discharged grids (Formvar/Carbon 300-mesh; Electron Microscopy Sciences, Hatfield, PA, USA) were treated with the resultant samples containing either A $\beta_{40}$  species, M-TTR species, or their mixture with or without ZnCl<sub>2</sub> (25  $\mu\text{M}$  for peptides, proteins, or ZnCl<sub>2</sub>; 5  $\mu\text{L}$ ) for 2 min at room temperature. Excess sample was removed using filter paper followed by washing with ddH<sub>2</sub>O three times. Each grid incubated with uranyl acetate (1% w/v, aq; 5  $\mu\text{L}$ ; Polysciences, Warrington, PA, USA) for 2 min at room temperature was blotted off and dried overnight at room temperature. The location of the samples on the grids was randomly picked, taking more than 20 images per grid.

**Cell Viability Studies.** The human neuroblastoma SH-SY5Y cell line was purchased from the American Type Culture Collection (Manassas, VA, USA). SH-SY5Y cells were maintained in the

media containing minimum essential medium (MEM, 50% v/v; GIBCO, Grand Island, NY, USA) and F-12 (50% v/v; GIBCO) supplemented with fetal bovine serum (FBS, 10% v/v; Sigma-Aldrich) and penicillin (100 U/mL) with streptomycin (100 mg/mL; GIBCO). The cells were grown and maintained at 37 °C in a humidified atmosphere with 5% CO<sub>2</sub>. Cell viability was determined by the MTT assay [MTT = 3-(4,5-dimethylthiazol-2-yl)-2,5-diphenyltetrazolium bromide; Biosesang, Seoul, Republic of Korea]. A $\beta$ <sub>40</sub> (125  $\mu$ M) and M-TTR (125  $\mu$ M) were preincubated with or without ZnCl<sub>2</sub> (125  $\mu$ M) for 24 h at 37 °C under quiescent conditions in 20 mM HEPES, pH 7.4, 150 mM NaCl. Cells were seeded in a 96-well plate (50,000 cells/100  $\mu$ L; SPL Life Sciences, Pocheon, Gyeonggi, Republic of Korea) and treated with the samples (final concentrations, 25  $\mu$ M for peptides, proteins, or ZnCl<sub>2</sub>). After 24 h incubation, the cells were washed with PBS (pH 7.4) and the media. MTT [5 mg/mL in PBS (pH 7.4); 25  $\mu$ L] was added to each well, and the plate was incubated for 4 h at 37 °C. Formazan produced by cells was solubilized using an acidic solution of *N,N*-dimethylformamide (pH 4.5, 50% v/v, aq; Daejung Chemicals, Busan, Republic of Korea) and SDS (20% w/v; Wako Chemicals) at room temperature overnight in the dark. Absorbance was measured at 600 nm by a microplate reader (Molecular Devices). Cell viability was calculated, compared to that of the cells treated with an equivalent amount of the buffered solution. Data are presented as mean  $\pm$  s.e.m. for  $n = 6$  examined over three independent experiments. For the statistical analysis, Student's *t*-test was used.

**Electronic Abs Spectroscopy.** To obtain the  $K_d$  value of Zn(II)–M-TTR and Zn(II)–Zincon (2-carboxy-2'-hydroxy-5'-sulfoformazyl-benzene monosodium salt; Alfa Aesar) in 20 mM HEPES, pH 7.4, 150 mM NaCl, the solution of Zincon (25  $\mu$ M; 0.5% v/v DMSO) was titrated with ZnCl<sub>2</sub> (2.5–100  $\mu$ M) in the absence and presence of M-TTR (10  $\mu$ M). The alteration in Abs at 618 nm in the presence of M-TTR was plotted as a function of [Zn(II)]/[M-TTR] to estimate the Zn(II)-to-M-TTR binding stoichiometry. The  $K_d$  value was determined by the HypSpec program (Protonic Software, Leeds, UK).<sup>5,6</sup> Data are presented as mean  $\pm$  s.e.m. for  $n = 2$ . To evaluate the potential contribution of multiple Zn(II)-binding events in M-TTR to the  $K_d$  determination and cooperativity, a mixture of ZnCl<sub>2</sub> (12.5  $\mu$ M) and Zincon (25  $\mu$ M; 0.5% v/v DMSO) was titrated with M-TTR (1–13  $\mu$ M), and the Hill coefficient was calculated following the Hill's equation.<sup>7</sup>

**2D <sup>1</sup>H–<sup>15</sup>N HSQC NMR Spectroscopy.** The solution of uniformly <sup>15</sup>N-labeled A $\beta$ <sub>40</sub> (35  $\mu$ M) with and without Zn(II) (35  $\mu$ M) and M-TTR (35  $\mu$ M) was prepared in 50 mM HEPES, pH 7.4 (7% D<sub>2</sub>O). For the preparation of samples containing M-TTR, EDTA (5 mM), and DTT (5 mM) were first

treated to the solution of M-TTR, followed by an extensive buffer exchange with the buffered solution. The sample was transferred to a 5-mm Shigemi NMR tube (300  $\mu$ L; Sigma-Aldrich). All the NMR experiments were conducted at 10 °C. Experimental data were acquired and processed by the TopSpin 3.2 software package (Bruker), and then analyzed using the POKY software suite.<sup>8</sup> The <sup>1</sup>H and <sup>15</sup>N assignments of <sup>15</sup>N-labeled A $\beta$ <sub>40</sub> were determined based on the previous results.<sup>3</sup>

**ESI-MS, ESI-MS<sup>2</sup>, and LC-MS.** A $\beta$ <sub>40</sub> (100  $\mu$ M) was incubated with M-TTR (100  $\mu$ M) in the absence and presence of ZnCl<sub>2</sub> (100  $\mu$ M) for 3 h or 24 h at 37 °C under quiescent conditions in 20 mM ammonium acetate, pH 7.4 (Sigma-Aldrich). Before injection into the mass spectrometer, the resultant samples were diluted 10-fold with LC-grade H<sub>2</sub>O. The capillary voltage, the drying gas flow, and the gas temperature were set to 5.8 kV, 12 L/min, and 300 °C, respectively. The ESI parameters and experimental conditions for ESI-MS<sup>2</sup> were same as above. The collision-induced dissociation was conducted by applying the collision energy at 35–50 eV. The measurements were conducted in triplicate. For LC-MS experiments, formic acid (0.1% v/v, aq, solvent A; 0.1% v/v, acetonitrile, solvent B) was used for gradient elution (5%, 50%, and 95% solvent B were used at 0 min, 50 min, and 51 min, respectively). Extracted ion chromatograms for target masses corresponding to A $\beta$  fragments were obtained with a mass error of  $\pm$  0.5 Da error.

**Cross-linking Experiments.** Samples were prepared following the procedures described in TEM. Peptides and proteins in the resultant samples (25  $\mu$ L) were cross-linked by adding glutaraldehyde (25% w/w, aq; 1  $\mu$ L; Daejung Chemicals) for 2 min at room temperature.<sup>9</sup> To quench the reactions, NaBH<sub>4</sub> (7% w/v; TCI) in 0.5 M NaOH (aq; Daejung Chemicals) (1  $\mu$ L) was mixed with the samples for 1 min at room temperature.<sup>9</sup> Each sample (5  $\mu$ L) was denatured with SDS (5% w/v; 5  $\mu$ L; Wako Chemicals) and heated for 5 min at 95 °C. The resultant samples were resolved through the homemade gel (5% w/v acrylamide for stacking gels; 12% w/v acrylamide for resolving gels; 10% w/v SDS). Following separation, the peptides and proteins were transferred onto nitrocellulose membranes and blocked with bovine serum albumin (BSA, 3% w/v; Sigma-Aldrich) in Tris-buffered saline (TBS) containing 0.1% v/v Tween-20 (Sigma-Aldrich) (TBS-T) for 4 h at room temperature or overnight at 4 °C. The membranes were incubated with an anti-A $\beta$  antibody (6E10; 1:20,000; Biolegend, San Diego, CA, USA) or an anti-TTR antibody (1:3,000; Thermo Fisher Scientific, Waltham, MA, USA) in the solution of BSA (2% w/v in TBS-T) at room

temperature (4 h for 6E10; 1 h for the anti-TTR antibody). After washing with TBS-T three times (10 min), a horseradish peroxidase-conjugated goat anti-mouse (1:7,500 for 6E10; Cayman, Ann Arbor, MI, USA) or anti-rabbit (1:15,000 for anti-TTR; Promega, Madison, WI, USA) secondary antibody in the solution of BSA (2% w/v in TBS-T) was added for 1 h at room temperature. After washing with TBS-T three times (10 min), a homemade ECL kit<sup>10</sup> was used to visualize the images gained by gel/Western blot on a ChemiDoc MP Imaging System (Bio-Rad). The measurements were conducted in triplicate.

**Table S1** Fitting parameters and mean squared residual error obtained from the global fitting of kinetic models to the experimental data shown in Fig. 1c and S6.

			Upper bound	Lower bound
<b>Zn(II)-A<math>\beta</math><sub>40</sub></b>	<b><math>k_1 k_n</math> (M<sup>-2</sup>s<sup>-2</sup>)</b>	$5.5 \times 10^9$	$8.3 \times 10^7$	$6.0 \times 10^7$
	<b><math>n_c</math></b>	2	–	–
	<b>MRE</b>	0.0036	–	–
<b>Metal-free A<math>\beta</math><sub>40</sub></b>	<b><math>k_1 k_n</math> (M<sup>-2</sup>s<sup>-2</sup>)</b>	$1.1 \times 10^6$	$2.7 \times 10^4$	$2.5 \times 10^4$
	<b><math>k_1 k_2</math> (M<sup>-3</sup>s<sup>-2</sup>)</b>	$5.8 \times 10^{14}$	$2.2 \times 10^{13}$	$1.3 \times 10^{13}$
	<b><math>K_M</math> (M<sup>2</sup>)</b>	$4.9 \times 10^{-12}$	$1.2 \times 10^{-13}$	$2.4 \times 10^{-13}$
	<b><math>n_c</math></b>	2	–	–
	<b><math>n_2</math></b>	2	–	–
	<b>MRE</b>	0.0095	–	–

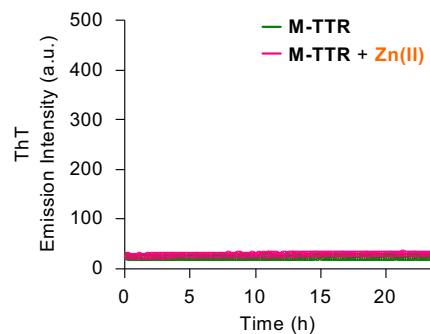


**Fig. S1** Aggregation kinetics of M-TTR with and without Zn(II) treatment monitored by the ThT assay. Conditions: [M-TTR] = 25  $\mu$ M; [ZnCl<sub>2</sub>] = 25  $\mu$ M; 20 mM HEPES, pH 7.4, 150 mM NaCl; 37 °C; quiescent conditions;  $\lambda_{\text{ex}}$  = 440 nm;  $\lambda_{\text{em}}$  = 490 nm. The error bars denote s.e.m. for  $n = 9$  examined over three independent experiments.

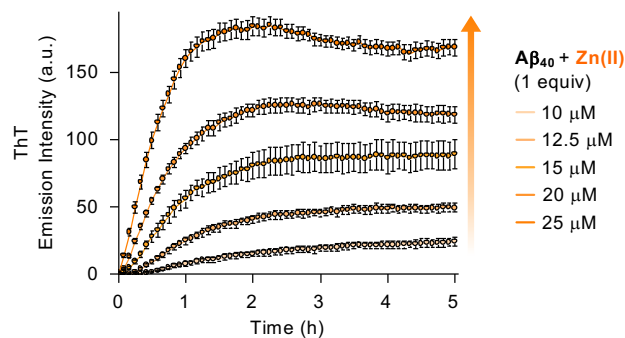


**Fig. S2** Aggregation profile of A $\beta_{40}$  in the presence of equimolar Zn(II). Conditions: [A $\beta_{40}$ ] = 10–25  $\mu$ M; [ZnCl $_2$ ] = 10–25  $\mu$ M; 20 mM HEPES, pH 7.4, 150 mM NaCl; 37  $^{\circ}$ C; quiescent conditions;  $\lambda_{\text{ex}}$  = 440 nm;  $\lambda_{\text{em}}$  = 490 nm. The error bars denote s.e.m. for  $n$  = 9 examined over three independent experiments.

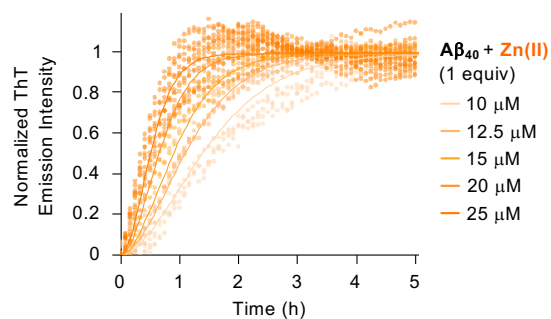


**Fig. S3** Normalized aggregation curves of  $A\beta_{40}$  in the presence of equimolar  $Zn(II)$  with the global fitting of the secondary nucleation model involving primary nucleation, elongation, and secondary nucleation steps. The data were reasonably fitted (solid lines) with the following fitting parameters and MRE:  $k_+k_n$ ,  $6.3 \times 10^9 \text{ M}^{-2}\text{s}^{-2}$  with  $1.2 \times 10^8 \text{ M}^{-2}\text{s}^{-2}$  and  $2.2 \times 10^8 \text{ M}^{-2}\text{s}^{-2}$  for upper and lower bounds, respectively;  $k_+k_2$ ,  $6.1 \times 10^{14} \text{ M}^{-3}\text{s}^{-2}$  with  $5.6 \times 10^{13} \text{ M}^{-3}\text{s}^{-2}$  and  $3.4 \times 10^{13} \text{ M}^{-3}\text{s}^{-2}$  for upper and lower bounds, respectively; reaction order for primary nucleation ( $n_c$ ), 2; reaction order for secondary nucleation ( $n_2$ ), 2; MRE, 0.0044.

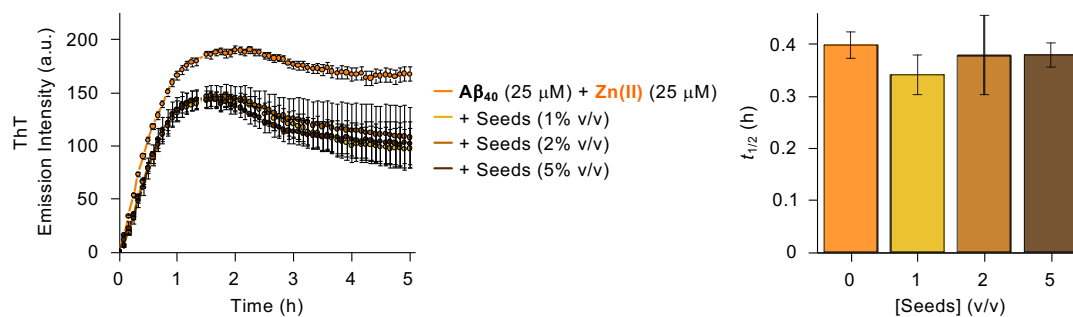


**Fig. S4** Aggregation kinetics of Zn(II)-added A $\beta_{40}$  in the presence of seeds traced by the ThT assay. The  $t_{1/2}$  values were obtained from the aggregation curves and plotted as a function of [seeds]. Conditions: [A $\beta_{40}$ ] = 25  $\mu$ M; [ZnCl<sub>2</sub>] = 25  $\mu$ M; 1, 2, and 5% v/v Zn(II)-treated A $\beta_{40}$  seeds. 20 mM HEPES, pH 7.4, 150 mM NaCl; 37 °C; quiescent conditions;  $\lambda_{\text{ex}}$  = 440 nm;  $\lambda_{\text{em}}$  = 490 nm. The error bars denote s.e.m. for  $n = 9$  examined over three independent experiments.

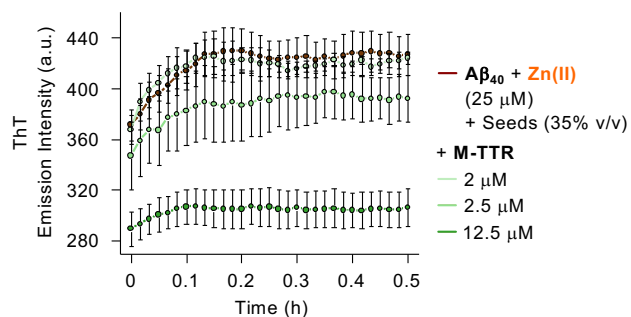


**Fig. S5** Aggregation curves of Zn(II)-treated A $\beta$ <sub>40</sub> in the presence of seeds investigated by the ThT assay. Conditions: [A $\beta$ <sub>40</sub>] = 25  $\mu$ M; [M-TTR] = 2–12.5  $\mu$ M; [ZnCl<sub>2</sub>] = 25  $\mu$ M; 35% v/v Zn(II)-treated A $\beta$ <sub>40</sub> seeds; 20 mM HEPES, pH 7.4, 150 mM NaCl; 37 °C; quiescent conditions;  $\lambda_{\text{ex}}$  = 440 nm;  $\lambda_{\text{em}}$  = 490 nm. The error bars denote s.e.m. for  $n$  = 9 examined over three independent experiments.

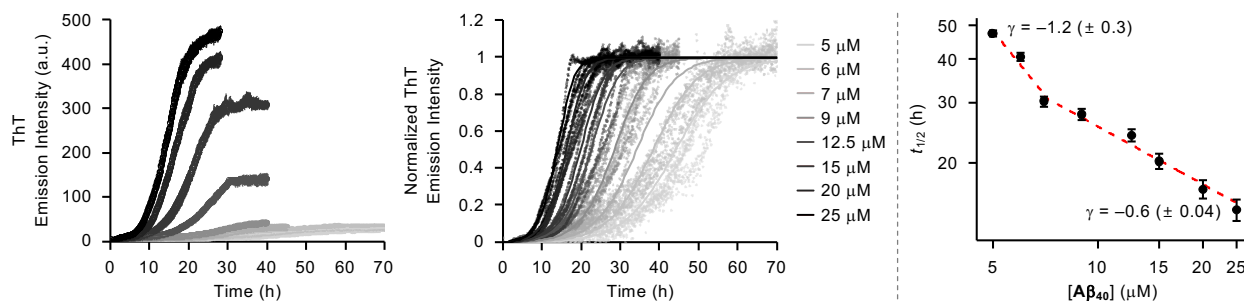


**Fig. S6** Aggregation kinetics of metal-free A $\beta_{40}$  observed by the ThT assay. The aggregation curves (left) were normalized for global fitting of kinetic models (middle), and the  $t_{1/2}$  value of each curve was plotted as a function of [A $\beta_{40}$ ] to obtain scaling exponents ( $\gamma$ ) (right). The data were well-fitted to the multistep secondary nucleation model (middle; solid lines). Conditions: [A $\beta_{40}$ ] = 5–25  $\mu$ M; 20 mM HEPES, pH 7.4, 150 mM NaCl; 37 °C; quiescent conditions;  $\lambda_{ex}$  = 440 nm;  $\lambda_{em}$  = 490 nm. The error bars denote s.e.m. for  $n$  = 9 examined over three independent experiments.

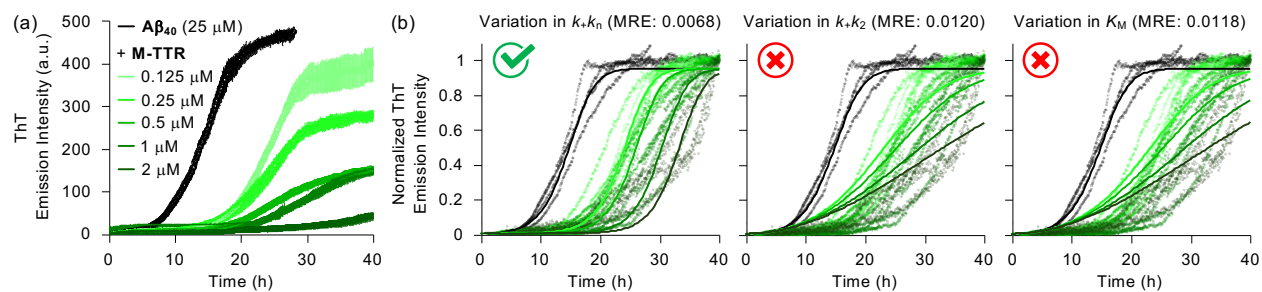


**Fig. S7** Effect of M-TTR on the aggregation kinetics of metal-free Aβ<sub>40</sub> analyzed by the ThT assay. (a) Aggregation curves of metal-free Aβ<sub>40</sub> with various [M-TTR]. Conditions: [Aβ<sub>40</sub>] = 25 μM; [M-TTR] = 0.125–2 μM; 20 mM HEPES, pH 7.4, 150 mM NaCl; 37 °C; quiescent conditions; λ<sub>ex</sub> = 440 nm; λ<sub>em</sub> = 490 nm. The error bars denote s.e.m. for *n* = 9 examined over three independent experiments. (b) Normalization of the aggregation curves shown in Fig. S7a for global fitting of the multistep secondary nucleation model with variations in *k*+*k*<sub>*n*</sub>, *k*+*k*<sub>*2*</sub>, and *K*<sub>*M*</sub> values (solid lines). The values of MRE are presented to compare the goodness of different fits to the same data set.

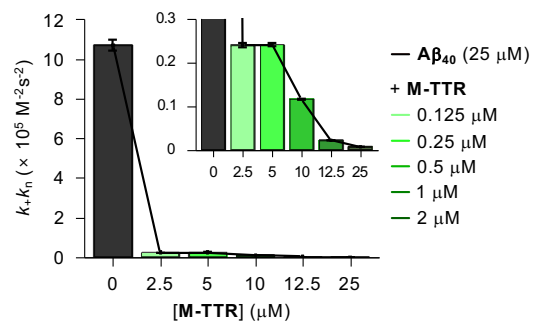


**Fig. S8** Change in the combined rate constant,  $k+k_n$ , of  $\text{A}\beta_{40}$  aggregation upon addition of M-TTR without Zn(II) treatment.

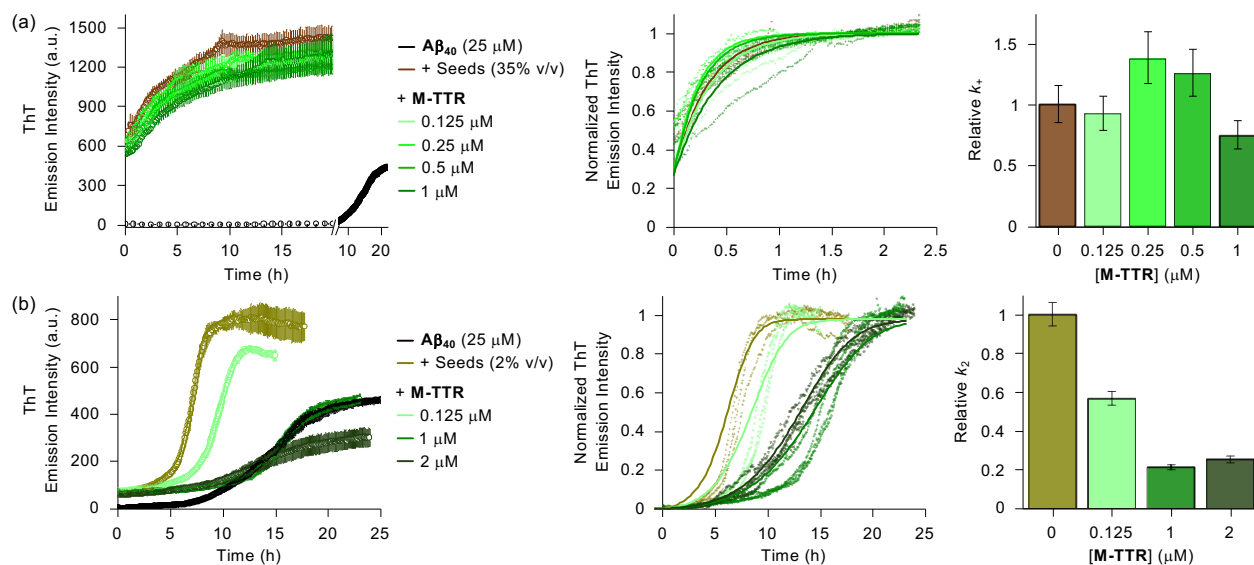


**Fig. S9** Aggregation kinetics of metal-free  $A\beta_{40}$  in the absence and presence of M-TTR with (a) 35% v/v or (b) 2% v/v seeds. The aggregation curves (left) were normalized for the global fitting of the multistep secondary nucleation model (middle; solid lines). The alteration in rate constants of metal-free  $A\beta_{40}$  aggregation [elongation for (a); secondary nucleation for (b)] was plotted as a function of [M-TTR] (right). Conditions:  $[A\beta_{40}] = 25 \mu\text{M}$ ;  $[M-TTR] = 0.125\text{--}1 \mu\text{M}$  [for (a)] or  $0.125\text{--}2 \mu\text{M}$  [for (b)]; 2% or 35% v/v  $A\beta_{40}$  seeds. 20 mM HEPES, pH 7.4, 150 mM NaCl; 37 °C; quiescent conditions;  $\lambda_{\text{ex}} = 440 \text{ nm}$ ;  $\lambda_{\text{em}} = 490 \text{ nm}$ . The error bars denote s.e.m. for  $n = 9$  examined over three independent experiments.

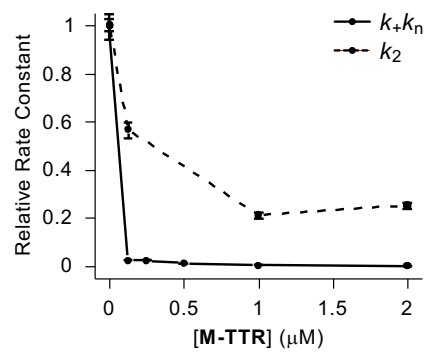


**Fig. S10** Change in rate constants [ $k+k_n$  (solid line) and  $k_2$  (dashed line)] of metal-free  $\text{A}\beta_{40}$  aggregation upon treatment of M-TTR obtained from the aggregation curves shown in Fig. S7 and S9b.

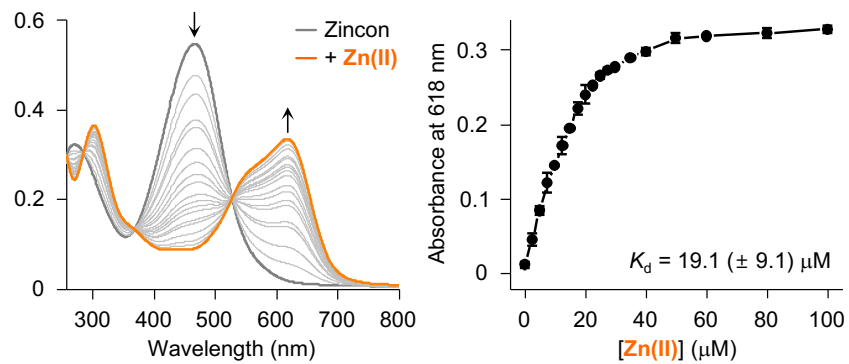


**Fig. S11** Determination of the  $K_d$  value for the Zn(II)–Zincon complex. The titration experiments were performed by electronic Abs spectroscopy to monitor the Abs change of Zincon at 618 nm upon addition of various [Zn(II)] and estimate the  $K_d$  value. Data are presented as mean  $\pm$  s.e.m. for  $n = 2$ . Conditions: [Zincon] = 25  $\mu\text{M}$ ; [ZnCl<sub>2</sub>] = 2.5–100  $\mu\text{M}$ ; 20 mM HEPES, pH 7.4, 150 mM NaCl; room temperature.

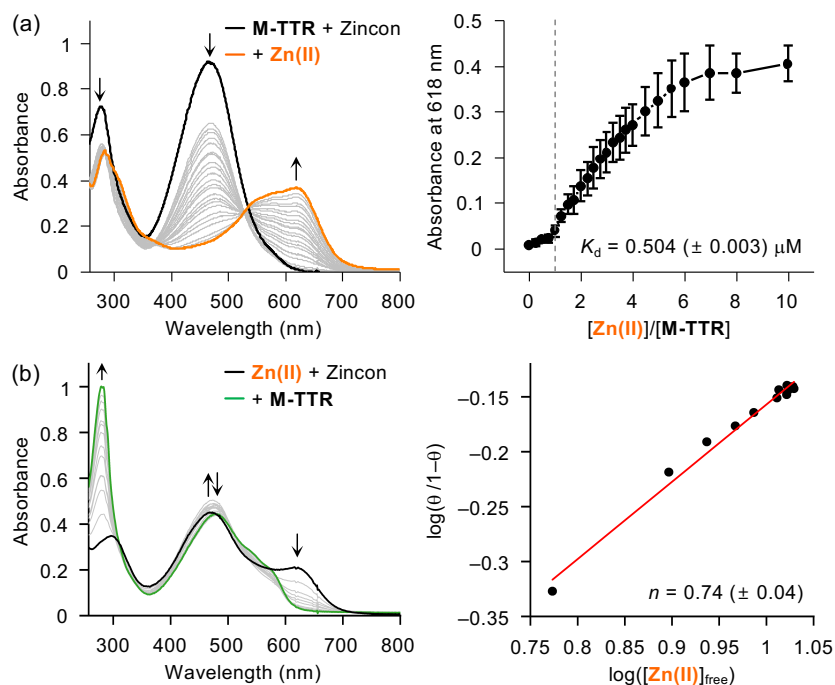


**Fig. S12** Titration experiments by electronic Abs spectroscopy to obtain the  $K_d$  value and Hill coefficient ( $n$ ) for Zn(II) binding towards M-TTR. (a) Electronic Abs spectra of the solution containing M-TTR and Zincon with varying concentrations of Zn(II). The change in Abs at 618 nm was plotted as a function of  $[Zn(II)]/[M-TTR]$  to estimate the Zn(II)-to-M-TTR binding stoichiometry and binding affinity. Data are presented as mean  $\pm$  s.e.m. for  $n = 3$ . Conditions:  $[M-TTR] = 10 \mu M$ ;  $[Zincon] = 25 \mu M$ ;  $[ZnCl_2] = 2.5-100 \mu M$ ; 20 mM HEPES, pH 7.4, 150 mM NaCl; room temperature. (b) Electronic Abs spectra of the solution of Zn(II) and Zincon titrated with M-TTR and the corresponding Hill plot. The  $\theta$  indicates the fraction of Zn(II) bound to M-TTR. The  $n$  value was calculated by fitting the data to Hill's equation<sup>7</sup> (red line) to determine the cooperativity of Zn(II) binding to M-TTR. Data are presented as mean  $\pm$  s.e.m. for  $n = 3$ . Conditions:  $[M-TTR] = 1-13 \mu M$ ;  $[Zincon] = 25 \mu M$ ;  $[ZnCl_2] = 12.5 \mu M$ ; 20 mM HEPES, pH 7.4, 150 mM NaCl; room temperature.

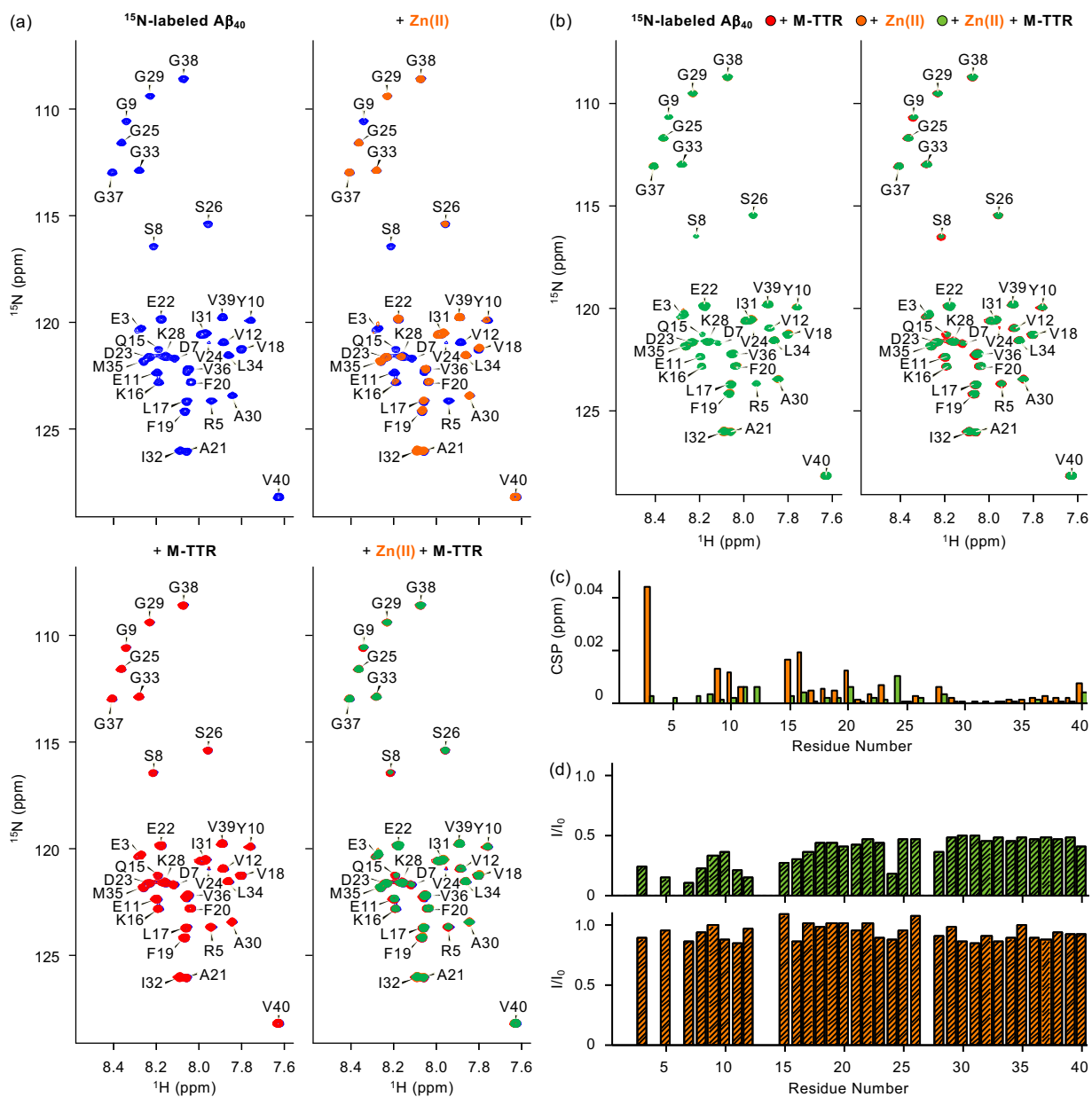


**Fig. S13** Interactions of M-TTR with Aβ<sub>40</sub> in the absence and presence of Zn(II). (a) 2D <sup>1</sup>H-<sup>15</sup>N HSQC NMR (850 MHz) spectra of <sup>15</sup>N-labeled Aβ<sub>40</sub> treated with either Zn(II), M-TTR, or both. Conditions: [<sup>15</sup>N-labeled Aβ<sub>40</sub>] = 35 μM; [M-TTR] = 35 μM; [ZnCl<sub>2</sub>] = 35 μM; 50 mM HEPES, pH 7.4; 7% v/v D<sub>2</sub>O; 10 °C. (b) 2D <sup>1</sup>H-<sup>15</sup>N HSQC NMR spectra of Zn(II)-added <sup>15</sup>N-labeled Aβ<sub>40</sub> with and without M-TTR (left) and M-TTR-treated <sup>15</sup>N-labeled Aβ<sub>40</sub> with and without Zn(II) (right). (c) CSPs of amino acid residues in <sup>15</sup>N-labeled Aβ<sub>40</sub> upon treatment of Zn(II) with (green) and without (orange) M-TTR. (d) Peak intensity ratios (I/I<sub>0</sub>) of amino acid residues in M-TTR-added <sup>15</sup>N-labeled Aβ<sub>40</sub> upon addition of Zn(II) (top) and <sup>15</sup>N-labeled Aβ<sub>40</sub> upon treatment of M-TTR (bottom).

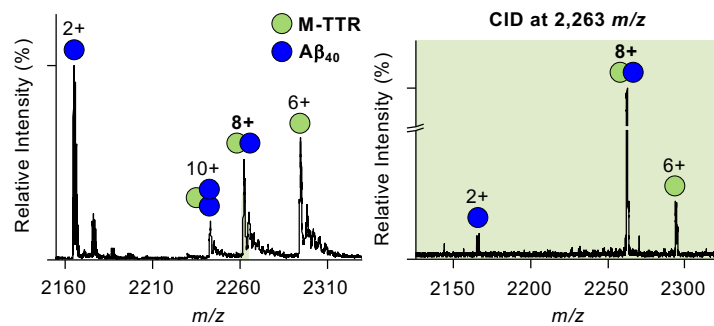


**Fig. S14** M-TTR binding to A $\beta_{40}$  in the absence of Zn(II) monitored by ESI-MS and ESI-MS<sup>2</sup>. Charge states are marked above the peaks in the spectra. Conditions: [A $\beta_{40}$ ] = 100  $\mu$ M; [M-TTR] = 100  $\mu$ M; 20 mM ammonium acetate, pH 7.4; 37  $^{\circ}$ C; 3 h incubation; quiescent conditions. The samples were diluted 10-fold before injection into the mass spectrometer. The measurements were conducted in triplicate.

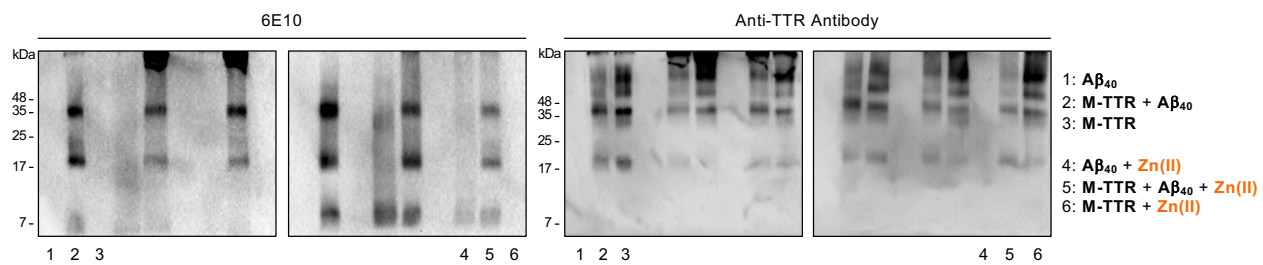


**Fig. S15** Original gel images from Fig. S16.

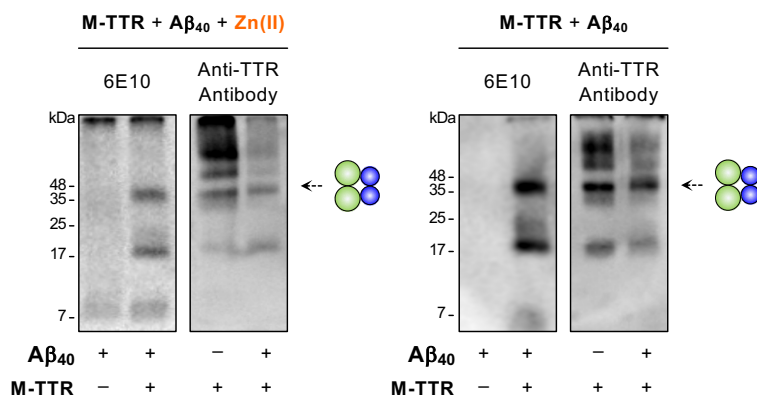


**Fig. S16** Size distribution of the cross-linked aggregates of M-TTR and A $\beta_{40}$  with or without Zn(II) analyzed by SDS-PAGE with Western blotting using anti-A $\beta$  (6E10) and anti-TTR antibodies. The assemblies highlighted in green and blue circles indicate heterotetramers composed of dimeric M-TTR and dimeric A $\beta_{40}$ , respectively. The original gel images are shown in Fig. S15. Conditions: [A $\beta_{40}$ ] = 25  $\mu$ M; [M-TTR] = 25  $\mu$ M; [ZnCl<sub>2</sub>] = 25  $\mu$ M; 20 mM HEPES, pH 7.4, 150 mM NaCl; 37 °C; 24 h incubation; quiescent conditions. The measurements were performed in triplicate.

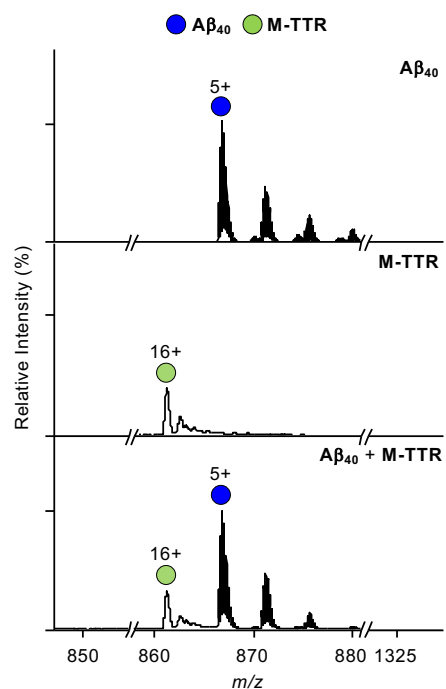


**Fig. S17** Mass spectra of Aβ<sub>40</sub>, M-TTR, and Aβ<sub>40</sub> with M-TTR. Charge states are marked above the peaks in the spectra. Conditions: [Aβ<sub>40</sub>] = 100 μM; [M-TTR] = 100 μM; 20 mM ammonium acetate, pH 7.4; 37 °C; 24 h incubation; quiescent conditions. The samples were diluted 10-fold before injection into the mass spectrometer. The measurements were conducted in triplicate.

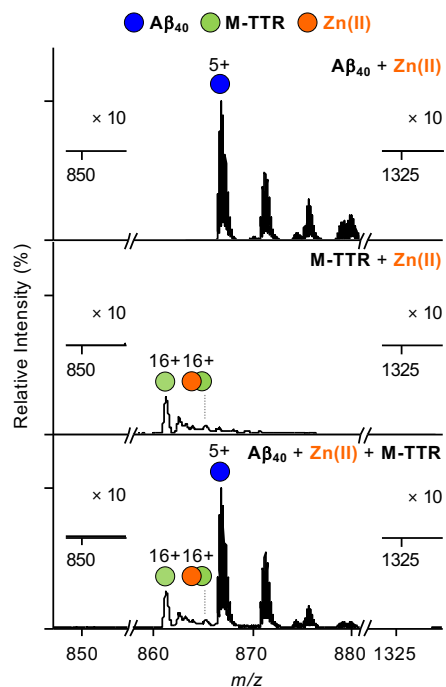


**Fig. S18** Mass spectra of Zn(II)-treated  $A\beta_{40}$ , M-TTR, and  $A\beta_{40}$  with M-TTR. Charge states are marked above the peaks in the spectra. Conditions:  $[A\beta_{40}] = 100 \mu\text{M}$ ;  $[M-TTR] = 100 \mu\text{M}$ ;  $[ZnCl_2] = 100 \mu\text{M}$ ; 20 mM ammonium acetate, pH 7.4; 37 °C; 3 h incubation; quiescent conditions. The samples were diluted 10-fold before injection into the mass spectrometer. The measurements were conducted in triplicate.

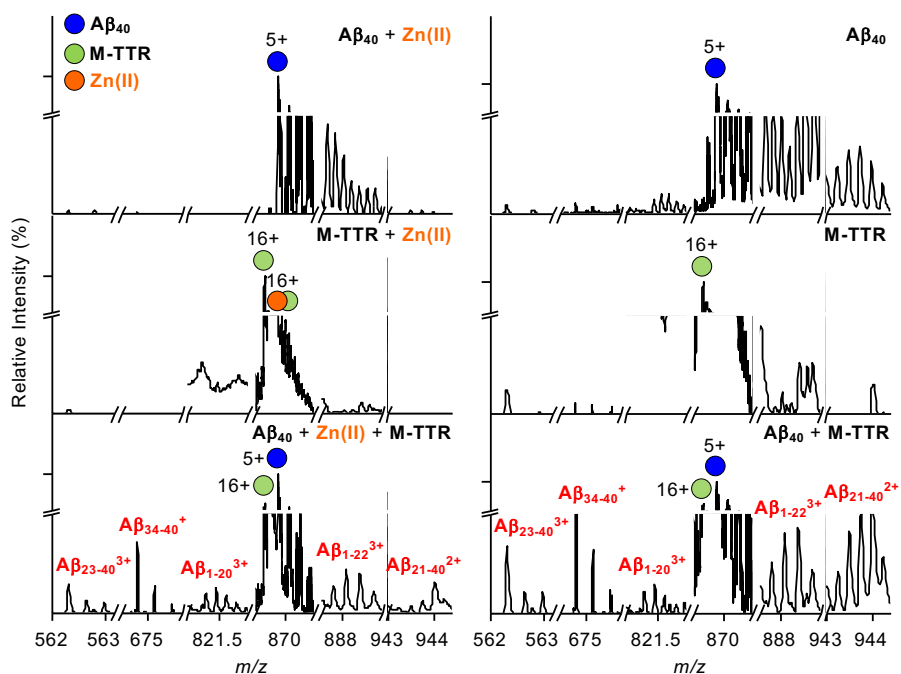


**Fig. S19** Aβ fragments generated upon treatment of M-TTR with Aβ<sub>40</sub> under Zn(II)-treated and -untreated conditions. Aβ fragments, including Aβ<sub>23-40</sub><sup>3+</sup> (563 *m/z*), Aβ<sub>34-40</sub><sup>+</sup> (674 *m/z*), Aβ<sub>1-20</sub><sup>3+</sup> (821 *m/z*), Aβ<sub>1-22</sub><sup>3+</sup> (888 *m/z*), and Aβ<sub>21-40</sub><sup>2+</sup> (944 *m/z*), were detected by ESI-MS. Charge states are marked above the peaks in the spectra. Conditions: [Aβ<sub>40</sub>] = 100 μM; [M-TTR] = 100 μM; [ZnCl<sub>2</sub>] = 100 μM; 20 mM ammonium acetate, pH 7.4; 37 °C; 24 h incubation; quiescent conditions. The samples were diluted 10-fold before injection into the mass spectrometer. The measurements were conducted in triplicate.

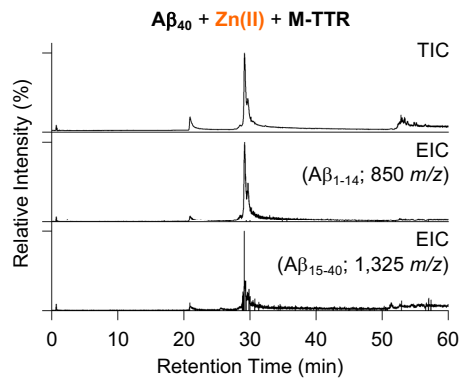


**Fig. S20** LC–MS analysis of the A $\beta$ <sub>40</sub> sample incubated with M-TTR in the presence of Zn(II). The total ion chromatogram (TIC) shows the summed intensity across 50–1,500 *m/z* detected for 60 min. Extracted ion chromatograms (EICs) were obtained for the A $\beta$ <sub>1-14</sub> and A $\beta$ <sub>15-40</sub> fragments generated upon treatment of A $\beta$ <sub>40</sub> with M-TTR under Zn(II)-treated conditions. Conditions: [A $\beta$ <sub>40</sub>] = 100  $\mu$ M; [M-TTR] = 100  $\mu$ M; [ZnCl<sub>2</sub>] = 100  $\mu$ M; 20 mM ammonium acetate, pH 7.4; 37 °C; 24 h incubation; quiescent conditions.

## References

1. J. Oroz, J. H. Kim, B. J. Chang and M. Zweckstetter, *Nat. Struct. Mol. Biol.*, 2017, **24**, 407.
2. B. I. Leach, X. Zhang, J. W. Kelly, H. J. Dyson and P. E. Wright, *Biochemistry*, 2018, **57**, 4421.
3. Y. Yi, Y. Lin, J. Han, H. J. Lee, N. Park, G. Nam, Y. S. Park, Y. H. Lee and M. H. Lim, *Chem. Sci.*, 2021, **12**, 2456.
4. G. Meisl, J. B. Kirkegaard, P. Arosio, T. C. Michaels, M. Vendruscolo, C. M. Dobson, S. Linse and T. P. J. Knowles, *Nat. Protoc.*, 2016, **11**, 252.
5. L. Alderighi, P. Gans, A. Ienco, D. Peters, A. Sabatini and A. Vacca, *Coord. Chem. Rev.*, 1999, **184**, 311.
6. P. Gans, A. Sabatini and A. Vacca, *Anal. Chim.*, 1999, **89**, 45.
7. A. Krężel and W. Maret, *Arch. Biochem. Biophys.*, 2016, **611**, 3.
8. W. Lee, M. Rahimi, Y. Lee and A. Chiu, *Bioinformatics*, 2021, **37**, 3041.
9. J. Du and R. M. Murphy, *Biochemistry*, 2010, **49**, 8276.
10. D. D. Mruk and C. Y. Cheng, *Spermatogenesis*, 2011, **1**, 121.